Multipole Surface Plasmon Resonances in Conductively Coupled Metal Nanowire Dimers

Ina Alber,[†,*] Wilfried Sigle,[‡] Frank Demming-Janssen,[§] Reinhard Neumann,[†] Christina Trautmann,[†,⊥] Peter A. van Aken,[‡] and Maria Eugenia Toimil-Molares[†,*]

[†]Materials Research Department, GSI Helmholtzzentrum für Schwerionenforschung GmbH, Darmstadt, Germany, [‡]Stuttgart Center for Electron Microscopy, MPI for Intelligent Systems, Stuttgart, Germany, [§]CST-Computer Simulation Technology AG, Darmstadt, Germany, and [⊥]Department of Materials- and Geo-Sciences, Technische Universität Darmstadt, Darmstadt, Germany

ABSTRACT We report on the experimental and the theoretical investigation of multipole surface plasmon resonances in metal nanowires conductively connected by small junctions. The influence of a conductive junction on the resonance energies of nanowire dimers was simulated using the finite element method based software CST Microwave Studio and experimentally measured by electron energy-loss spectroscopy in a transmission electron microscope. We extend the analysis of conductively connected structures to higher order multipole modes up to third order, including dark modes. Our results reveal that an increase in junction size does not shift significantly the antibonding modes, but causes a strong blue shift of the bonding modes, leading to an energetic rearrangement of the modes compared to those of a capacitively coupled dimer with similar dimensions.

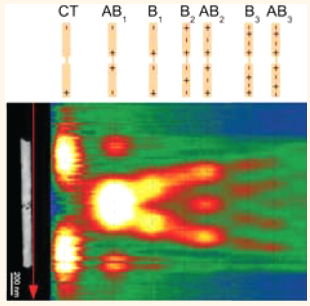

KEYWORDS: multipole order surface plasmon · nanowire dimer · conductive junction · electron energy-loss spectroscopy · finite element simulation · bonding mode · antibonding mode

Surface plasmon (SP) resonances excited in nanowire dimers have been recently studied very extensively due to their great potential for applications as surface-enhanced Raman spectroscopy[1−4] and surface-enhanced infrared spectroscopy.[5,6] Such a dimer consists of two nanowires separated by a gap of typically a few nanometers. The SP modes of the two individual nanowires couple capacitively *via* the gap, resulting in the formation of bonding and antibonding modes.[7−10] A bonding mode is characterized by an electric field distribution where electric field maxima of opposite sign are located at opposite gap sides. By the excitation of this mode, very high near-field enhancement is created at the position of the gap.[7] In contrast, the excitation of an antibonding mode creates electric field maxima of the same sign at opposite gap sites. These modes are hardly excitable using an incoming plane wave. Due to their low radiative losses, their application in light-guiding processes has been suggested.[11]

However, systematic studies on nanowire dimers with well-controlled nanowire dimensions and gap width are rare, due to the challenging preparation process of such structures. We recently synthesized nanowire dimers by pulsed electrodeposition of segmented Au/Ag/Au nanowires in etched ion-track membranes, followed by wet etching of the middle Ag segment to create a nanogap, and investigated the SP resonances of capacitively coupled nanowire dimers by electron energy loss spectroscopy (EELS) in a scanning transmission electron microscope (STEM).[12] If the dissolution of the Ag segment is not complete, the Au nanowires remain connected by a small metallic junction, influencing the SP resonance energies. Recent publications calculated the SP resonances of various conductively coupled nanostructures.[13−21] The authors report shifts of the resonance energies depending on junction size and conductivity and highlight the potential as interesting platforms to investigate the coupling between electronics and plasmonics as relevant, for example, for sensing and optical switching.[19,22]

In this paper, we investigate SP resonances of conductively and capacitively coupled μm-long metallic nanowire dimers, extending the analysis to higher order modes and including not only bright but also dark modes. CST Microwave Studio[23] calculations on Au nanowires are compared to experimental EELS-STEM results on conductively coupled AuAg alloy nanowires connected by junctions of different sizes that were synthesized by electrodeposition

* Address correspondence to i.alber@gsi.de, m.e.toimil-molares@gsi.de.

Received for review July 14, 2012 and accepted September 30, 2012.

Published online October 01, 2012
10.1021/nn303149p

in etched ion-track membranes. EELS-STEM is a suitable method for the analysis of SP modes, since it directly probes the local density of states of a nanostructure.[24] Applying EELS-STEM, it is possible to excite and investigate bright and dark modes in the dimer structures with a resolution of a few nanometers.[9,25]

RESULTS AND DISCUSSION

Figure 1 shows the electric field strength calculated for four different Au nanostructures: a continuous wire with length $L = 1145$ nm and diameter $D = 90$ nm (black line) and three nanowire dimers, each consisting of two wires with length $L = 563$ nm and diameter $D = 90$ nm. From top to bottom, the wires forming a dimer are either conductively connected by a cylindrical Au junction with length $l_j = 19$ nm and diameter $d_j = 40$ nm (blue line), conductively connected by a cylindrical Au junction with identical length and diameter $d_j = 20$ nm (green line), or separated by a 19 nm gap (red line). The end-caps of the structures have rounded edges with a radius of 11.3 nm. Schemes of the structures are depicted to the right of each spectrum. The spectra are shifted vertically for clarity and show the absolute value of the electric field strength measured at 1 nm distance from one end. The resonances are excited by a dipole located at 10 nm from the second end, oriented in the direction of the nanostructure axis. The electric field distributions of the different SP resonances are depicted schematically for a continuous wire (top) and for the capacitively coupled dimer (bottom).

These electric field distributions were obtained from calculations of the electric field at the corresponding SP resonance energies. Exemplarily, Figure 2a–f display two-dimensional plots of the *z*-electric field component (perpendicular to the depicted plane) for the dimer connected by a junction with $d_j = 20$ nm diameter (Figure 1, green line). Resonances are excited for all four structures at 0.82 ± 0.02, 1.55 ± 0.02, and 2.03 ± 0.02 eV (Figure 1, vertical dashed lines). At these energies, the resonances of all four structures have a symmetric field distribution with respect to the center of the wire. In the case of the capacitively coupled dimer (red spectrum), these resonances are denoted as antibonding modes. However, in the case of a continuous nanowire (black spectrum), they are assigned to the dark modes with multipole order $l = 2$, 4, and 6. Our results demonstrate that the resonance energies of these modes differ by only less than 0.04 eV for different junction sizes and that the symmetry is maintained for all four structures.

Figure 1 reveals for the dimer three further resonances, known as bonding modes of different l.[8] Modes with the same number of electric field maxima and similar field distribution to that for the bonding modes are found as well in the spectra of the two connected wires and the continuous wire. They are, in

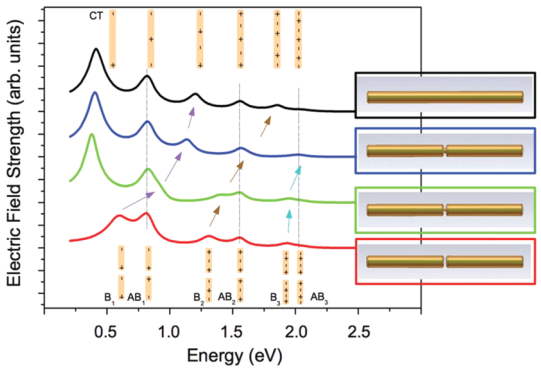

Figure 1. Absolute value of the electric field strength *versus* excitation energy for four different structures: a continuous wire with length 1145 nm (black line), a conductively coupled dimer with connection of length 19 nm and diameter 40 nm (blue line), a second conductively coupled dimer with the same connection length, but decreased connection diameter of 20 nm (green line), and a capacitively coupled dimer with gap 19 nm (red line).

the case of the continuous wire, assigned to the bright modes $l = 3$ and 5. We identify a clear blue shift of these resonances with increasing connection size, which is indicated by the arrows in Figure 1. The blue shift is attributed to the decreasing coupling strength between the modes of the two individual wires with increasing junction size. Calculations for two conductively connected gold nanoshells revealed the blue shift of the dipolar bonding mode with increasing conductance and junction size.[17,19] Here, the blue shift is demonstrated additionally for higher modes up to third order. Our analysis shows that resonances with similar asymmetric field distribution and the identical number of maxima are expected for all structures and that the resonance energy shifts to the blue with increasing junction size. In the case of the lowest multipole order, the shift to the blue of the resonance energy is even bigger than 0.6 eV. It is interesting to note that at a critical junction size AB and B modes are degenerate. In the framework of antenna theory this corresponds to a cancellation of capacitive and inductive load.[16]

Comparing in Figure 1 the spectra of the capacitively coupled dimer (red line) and the conductively coupled dimer ($d_j = 20$ nm) (green line), it becomes evident that the shift to the blue of the bonding modes when introducing a conductive junction is different for the first- and second-order resonances. In ref 17 the authors reported that the shift of the B_1-mode to higher energies occurs when the conductivity of the junction equals a certain threshold that allows the charges at the junctions to neutralize faster than the oscillation period of the corresponding SP mode. This implies that the conductivity threshold of the junction increases with the SP frequency. Thus, for a given junction (*e.g.*, $d_j = 20$ nm, green line), the shift in energy for the bonding modes depends on the mode order (*i.e.*, on the mode frequency), the blue shift being the

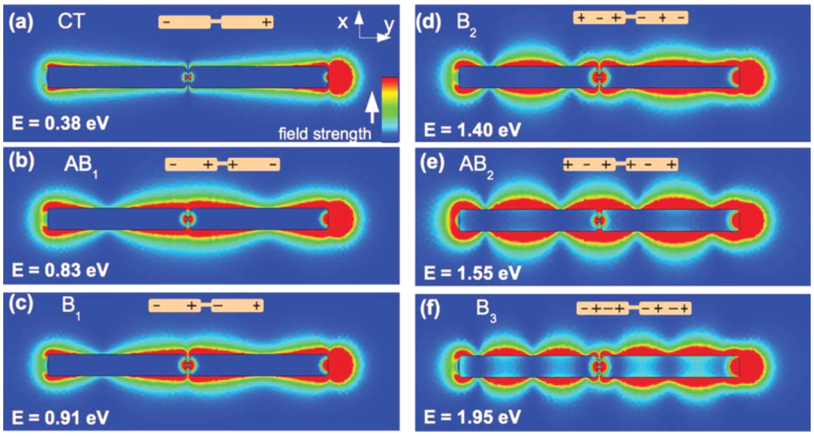

Figure 2. Electric field component in the direction perpendicular to the depicted plane (*z*-direction) in proximity to a nanowire dimer with a small connection of diameter 20 nm. The depicted plane is shifted by 8 nm in the *z*-direction. Red and blue color indicate high and low electric field, respectively. The excitation dipole is located to the right of the structures and is responsible for the high electric field (indicated by the red color) at this position.

largest for the B_1-mode and decreasing for B_2 and B_3 with increasing mode order. In addition, the larger the junction size, the larger is its conductivity, and thus the larger should be the shift for a given resonance energy. Interestingly, this frequency- or multipole-order-dependent shift of the resonances results in a mode rearrangement depending on the junction diameter. See for example the green spectrum, where the AB_1-mode is lower in energy than the B_1-mode, while in contrast the AB_2-mode is higher than the B_2-mode.

The resonance of lowest energy in the spectrum of the continuous wire is the charge transfer mode (CT). This mode is as well visible in the two spectra of the connected wires. It possesses a net charge in each of the two connected wires. Therefore, it can only be excited for the dimers if charge transfer between the two wires is possible.[15−17] Thus, the CT-mode does not exist for the capacitively coupled dimer system (red line). For the two connected dimers, the CT-mode reveals a weak blue-shift with increasing junction width (from 0.38 ± 0.01 to 0.40 ± 0.01 eV). For the continuous wire the corresponding CT-mode is further blue-shifted (0.41 ± 0.01 eV). This shift is assigned to the increased conductivity of the junction.

Figure 2 shows the calculated two-dimensional plots of the electric field *z*-component for the conductively coupled nanowire dimer (d_j = 20 nm) at the energies (a) 0.38, (b) 0.83, (c) 0.91, (d) 1.40, (e) 1.55, and (f) 1.95 eV. The color scale depicts the strength of the electric field at each position and is arbitrarily scaled for each image to optimize visualization of the maxima. The dipole is located at the right of the structures, and it is responsible for the high electric field at this position. The electric field is shown in an *x*−*y* plane shifted in the *z*-direction by 8 nm to the center plane of the structure. The electric field distributions are assigned to the SP modes resolved in Figure 1. For the antibonding modes at 0.83 and 1.55 eV a broad maximum is visible at the

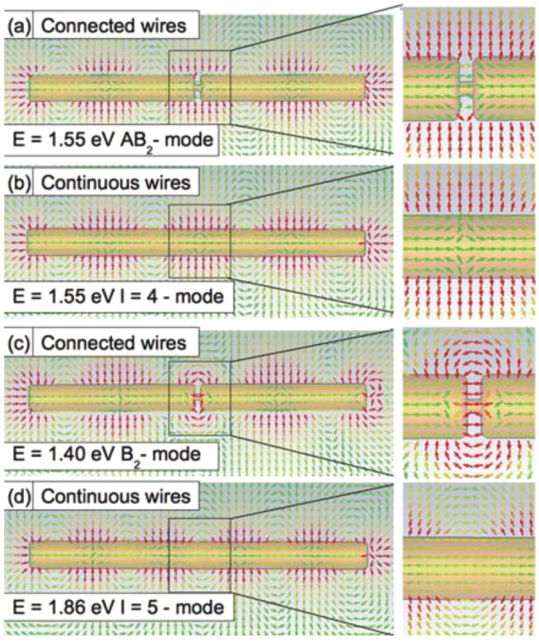

Figure 3. Calculated electric field for the AB_2-mode of a dimer with thin connection (a) and *l* = 4-mode of continuous wire (b), together with the electric field corresponding to the B_2-mode of connected dimer (c) and *l* = 5-mode of continuous wire (d). The direction of the arrows and the color depict the direction of the field and its strength. The details depict the center region with higher resolution.

structure center, while the three bonding modes (0.91, 1.40, and 1.95 eV) reveal two distinct maxima, one at each side of the nanowire ends close to the connection. The CT-mode at 0.38 eV does not have a maximum at the nanowire center.

As clearly visible in Figure 1, the antibonding resonance energies of the nanowire dimer structure do not shift significantly when adding conductive junctions of various sizes. Figure 3 shows the calculated two-dimensional plots of the electric field for the AB_2-mode of the dimer with thin connection (Figure 3a) together

with the one for the $l = 4$-mode of the continuous wire (Figure 3b). For comparison the field distributions for the B_2-mode of the conductively connected dimer (1.40 eV) and the $l = 5$-mode of the continuous wire (1.86 eV) are shown in Figure 3c and d. This Figure depicts the center plane of the structure, and the arrows indicate the direction of the electric field. The color of the arrows indicates the strength of the electric field and for each image is independently scaled to obtain the best visibility. The details show the gap region with higher resolution. Red color indicates high electric field, and green color low electric field. In the case of the AB_2-mode in Figure 3a the field close to the junction is very low. The field distribution of this mode is almost identical to the one of the continuous wire (Figure 3b). This is observed as well for the AB_1- and AB_3-modes (not shown in the figure). In contrast, for the B_2-mode at 1.40 eV a high electric field is excited in the gap (Figure 3c). This leads to a spatial shift of the electric field maxima in the direction of the structure center, compared to the position of the maxima of the $l = 5$-mode for the continuous wire (Figure 3d). Similar shifts of the maxima are observed for the B_1- and B_3-modes. The energy shifts with connection size of the bonding modes are thus attributed to the varying spatial field distributions. The antibonding modes, which have almost identical field distributions, are little shifted in energy. We conclude that the junction influences SP resonances only if a field is concentrated at the gap.

By pulsed electrodeposition in ion-track etched polycarbonate membranes Au-rich/Ag-rich/Au-rich segmented nanowires were synthesized. The diameter of the nanowires is determined by the pore size. The length of the segments is determined by the duration of the pulses. Complete or incomplete dissolution of the Ag-rich segment resulted in nanowire dimers separated by a gap or connected by a conductive junction, respectively. Details of the preparation of the connected dimers are presented in the Methods section. The SP resonances of these structures were experimentally investigated by EELS-STEM. While in the CST simulation the resonances are excited at one end of the structure and calculated for the second end, in the EELS measurement excitation and probe positions are identical. In EELS the energy loss of the incident beam is used to detect the SPs, since it depends on the electric field component in the direction of the velocity of the incoming electron beam.[24]

The TEM image in Figure 4a shows a conductively coupled nanowire dimer with total length 1145 ± 10 nm and diameter of 90 ± 10 nm. Unfortunately, the exact dimension and morphology of the junction cannot be determined from the TEM image. On the right side of the TEM image, an EELS map is shown. The map consists of 100 EEL spectra measured along the wire axis at approximately 15 nm distance from the

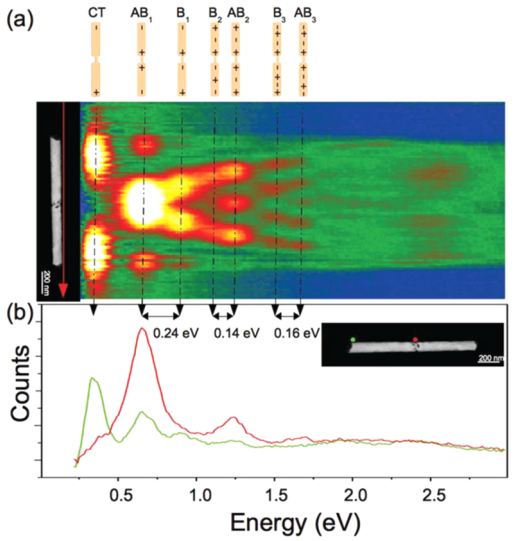

Figure 4. (a) Plasmonic EELS map of a nanowire dimer. The wires are connected by a conductive junction. The map consists of 100 EEL spectra that are measured along the red arrow in the TEM image on the left. The energy varies from left to right from 0.25 to 3.0 eV. The color indicates the number of counts. (b) Two spectra extracted from the intensity map in (a). The red curve shows a spectrum extracted from the middle of the map, while the green curve represents a spectrum extracted from one end of the structure (see red and green dots in the TEM image).

nanowire surface (red arrow). From left to right, the energy loss varies from 0.25 to 3.0 eV, and the color in the map indicates the number of counts. Blue color signifies low count number; white color indicates a high count number. Figure 4b shows two exemplary spectra extracted from the map at two different positions: close to the junction (red line) and close to one of the dimer edges (green line). The positions are indicated by the respective red and green dots in the TEM image on the right.

In the map, we can resolve seven different longitudinal SP modes at various energies. These modes are attributed to the modes identified in the simulations by counting the number of maxima along the structure (*i.e.*, along the dashed lines). Their corresponding charge distributions are presented schematically on top of the map.

The CT plasmon is depicted at an energy of 0.33 ± 0.02 eV and reveals the two characteristic intensity maxima at the two ends of the structure. The next two low-energy peaks can be attributed to the AB_1- and B_1-modes. In this case, the B_1-mode has a higher energy than the AB_1-mode. In contrast, the B_2- and B_3-modes are lower in energy than the AB_2- and AB_3-modes, respectively. These experimental results are in very good agreement with the presented simulations. It is important to notice that for the B_2- and B_3-modes, using EELS in a TEM, the maxima in the middle of the structure are not excited. This is due to the fact that the electron beam cannot excite an antisymmetric mode when placing the beam very close to the center

of the structure, as was already demonstrated in previous publications.[9,12,25] For the B_1-mode, the two maxima are not excited exactly at the center either. However, we can resolve these two maxima slightly away from the dimer center. We attribute this to the fact that for the low-order modes the maxima extend over a broader space than those of the high-order modes (see Figure 2).

We observe that the energy difference of the B_2- and AB_2-pair is smaller than that of the B_3- and AB_3-pair, in agreement with the simulations. This is in contrast to the results obtained for capacitively coupled dimers, for which decreasing energy differences between bonding and antibonding pairs with increasing multipole order were measured.[12]

Figure 5a shows the spectra of two conductively coupled nanowire dimers with similar aspect ratio, being $L/D = 13 \pm 1$, but different junction diameters. The dimensions of the two dimers are $L = 1145 \pm 10$ nm and $D = 90 \pm 10$ nm (Figure 4a, blue line) and $L = 1490 \pm 10$ nm, $D = 115 \pm 10$ nm, and $d_j = 30$ nm (green line), respectively. In contrast to all other wires presented here, this second dimer (green line) was annealed at 300 °C for half an hour. It was found that this procedure reduces the Ag content very slightly, by about 3−5%.

For both structures their antibonding modes are excited at very similar energies, marked with dashed black lines on the spectra. For the blue spectrum the AB_3-mode is not resolvable; however, its energy could be measured in Figure 4 and is additionally marked in the blue curve. The small deviations for the antibonding modes of the structures can be attributed to small deviations in aspect ratio, Ag content, and shape of the wires.[26] In contrast to these modes, the energies of the CT- and B_1-modes deviate much stronger, supporting the finding that the size of the junction only weakly influences the antibonding mode energies, while the CT-mode and the bonding modes depend clearly on its size. As expected, in the two spectra the CT-mode and the B1-mode of the structure with smaller junction have lower energies.

Figure 5b shows the spectra of two conductively coupled nanowire dimers with different aspect ratios. For one dimer it is $L/D = 20 \pm 3$, $L = 1510 \pm 10$ nm, $D = 75 \pm 10$ nm, and $d_j = 15$ nm (red line). For the second dimer (same as in Figure 5a (green line)) $L/D = 13 \pm 1$, $L = 1490 \pm 10$ nm, $D = 115 \pm 10$ nm, and $d_j = 30$ nm (green line). TEM images of the wires are depicted on top of the spectra, and the colored dots mark the measurement positions. The energies of all resolvable longitudinal modes in the red spectrum are red-shifted compared to the resonance energies in the green spectrum due to the larger aspect ratio of this wire. The energy difference between the B_1- and AB_1-modes is in this case bigger than that in the spectrum of the wire with smaller aspect ratio, although its junction is slightly smaller. This is due to a decreased conductivity

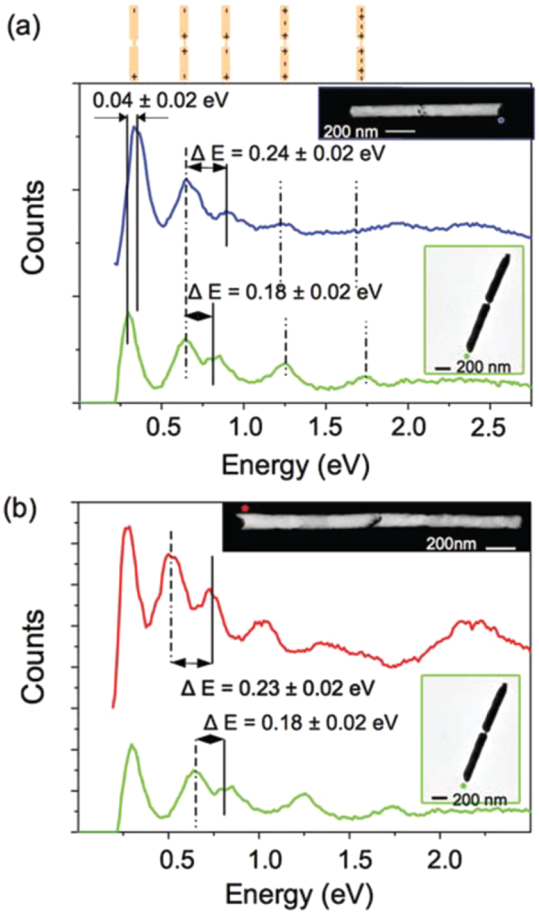

Figure 5. Spectra of conductively coupled nanowire dimers with small junctions. (a) The blue line corresponds to a spectrum of the nanostructure in Figure 4; the green line represents the spectrum of a nanowire dimer with a junction of thickness 30 nm. Both wires have similar aspect ratios of $L/D = 13 \pm 1$. (b) The red spectrum corresponds to a coupled dimer with $L/D = 20 \pm 3$ and a junction diameter of ~15 nm. The green line depicts the same spectrum as in (a). All spectra are measured at the positions of the colored dots in the TEM images.

threshold with decreased resonance energy, as discussed above. Remarkably, a broad peak, centered at an energy of about 2.2 eV, is resolved in the spectrum of the dimer with larger aspect ratio. This peak is not visible in the spectrum of the dimer with smaller aspect ratio. It is most probably due to a transversal mode of the structure. The fact that the transversal mode is visible only in the red spectrum can be understood from the different excitation positions indicated by the colored dots in the TEM images, indicating that the transversal modes can be excited parallel to the nanowire (red dot), but not along the continuation of the axis beyond the wire (green dot). This selective excitation of the transversal modes at positions parallel to the wire axis has been previously reported for single Au nanowires and Au nanowire dimers in ref 12.

After the Ag dissolution process, conductive junctions are found at different positions with respect to the nanowire axis. The conductive junctions in

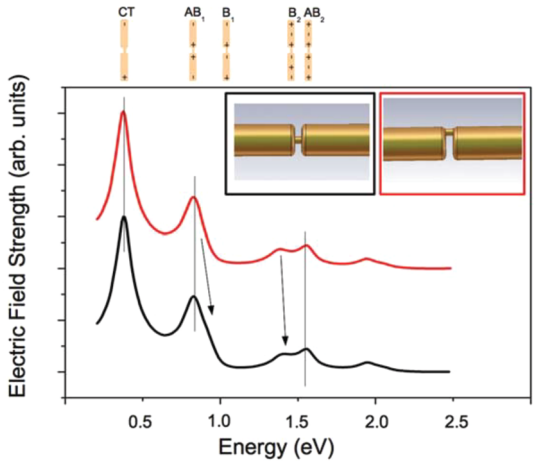

Figure 6. Calculated spectra of two nanostructures each consisting of conductively coupled nanowires with the same aspect ratio. The junction in both cases has the same diameter, d_j = 20 nm, and length, l_j = 19 nm. The black spectrum corresponds to a structure where the junction is located exactly in the middle of the structure, while the red spectrum corresponds to a structure with the junction shifted to the edge of the gap. The insets display the geometrical arrangement schematically.

Figure 5b are, for example, not centered. We have simulated the influence of the relative position of the conductive junction on the SP resonances. Figure 6 shows two spectra that are calculated for a dimer coupled conductively by a junction with l_j = 19 nm and d_j = 20 nm, placed either at the center (black line) or at the side (red line) of the two identical wires. The length and diameter of the complete structures are L = 1145 nm and D = 90 nm. The antibonding modes are excited at the same energies in both spectra. The low electric field at the position of the gap for the antibonding mode results in similar field distributions for both structures independent of the connection position. However, the resonance energies of the bonding modes differ slightly, being excited at higher energies for the structure connected at the middle. This demonstrates that not only the size but also the positioning of such a junction determines the bonding mode resonance energies.

CONCLUSIONS

We have investigated the SP resonance energies on conductively coupled metal nanowire dimers and compared them to those of an unconnected nanowire dimer and a continuous wire of similar dimensions. Our results extend the analysis of SP modes on conductively coupled nanostructures to multipole modes, including both bright and dark modes. We demonstrate theoretically and experimentally that modes with the same number of electric field maxima and symmetry exist in all four structures. The resonances with field distribution symmetrical to the center of the structures are in the case of the unconnected dimer denoted as the antibonding modes. Their resonance energies differ only very slightly for different junction sizes. In contrast, the resonances with antisymmetrical field distribution, known as bonding modes, reveal strong blue shifts. This is explained by the concentrated electric field at the position of the gap for the bonding modes, resulting in a spatial shift of the field maxima in the gap direction. For the antibonding modes the low field in the gap leads to almost identical field distributions for the dimers and the continuous wire. We find that the blue shift of the bonding modes decreases with increasing mode order, which can lead to an energetic rearrangement of the SP modes of conductively coupled dimers compared to capacitively coupled ones. For a fixed junction size, the arrangement of the modes of lower energy resembles that of the continuous wire. For example the B_1-mode is blue-shifted compared to the AB_1-mode. For modes of higher energy of the same structure the arrangement is that of a dimer, which means the B_2-mode is red-shifted to the AB_2-mode. For the CT plasmon a small blue-shift with increasing junction size is confirmed. Finally, the dependence of the resonance energies on the position of a small junction connecting the two wires has been investigated. Only very slight deviations in the resonance energy of the bonding modes are found for different positions.

METHODS

AuAg alloy nanowire dimers connected by junctions of varying size are synthesized. First, the nanowires are electrochemically deposited into the pores of ion-track etched polymer templates. Foils of thickness 30 μm are irradiated at the heavy ion accelerator UNILAC at GSI Helmholtz Center for Heavy Ion Research. Subsequently, chemical etching using 6 M NaOH at 50 °C transforms the ion tracks into nanochannels.[27−29] Nanowires are grown electrochemically in the channels at 60 °C using an electrolyte containing 20 mM $KAg(CN)_2$ and 50 mM $KAu(CN)_2$. A pulse sequence is applied during the deposition process to create an Ag-rich segment enclosed by two Au-rich segments. The Au-rich segments are deposited applying −1.1 V *versus* a Ag/AgCl reference electrode, while −0.5 V *versus* a Ag/AgCl reference electrode is applied for the Ag-rich segment. The duration of each pulse defines the length of the different segments. For the STEM analysis, the nanowires are drop-casted on a 30 nm thick silicon nitride membrane (Plano GmbH) and dipped into concentrated nitric acid for 3 h to etch away the Ag-rich segments.[30,31] EDX-SEM analysis reveals that after the nitric acid treatment the Au-rich segments possess a Au:Ag ratio of about 60:40. Due to the lower Ag concentration, Ag atoms are enclosed by Au atoms and cannot be etched away using nitric acid. Because of a small Au content in the Ag-rich parts, not all Ag-rich segments are completely dissolved (Au:Ag of about 15:85 measured by EDX:SEM). In some cases, a small junction is found between the two Au-rich segments.

STEM-EELS analysis was performed using the Zeiss SESAM transmission electron microscope operated at 200 kV with a field-emission gun and equipped with the MANDOLINE energy filter.[32] An electrostatic omega-type monochromator reduces the energy spread to 0.1 eV. The width is slightly increased to 0.12 eV for the present experiments to increase the electron

probe current and thus improve counting statistics. In all spectra, the zero-loss peak is subtracted by fitting a power law function to the positive energy-loss tail of this peak.

The simulation was performed using the frequency solver of CST Microwave Studio. The solver is based on the finite element method. All spectra are calculated for a distance of 1 nm from the Au structure. The excitation source is a small dipole, located at the other end of the structure with an impedance of 5 kΩ. The spectra are normalized to the electric field of the dipole at the specific position if no Au nanostructure is present.

Conflict of Interest: The authors declare no competing financial interest.

REFERENCES AND NOTES

1. Li, S.; Pedano, M. L.; Chang, S. H.; Mirkin, C. A.; Schatz, G. C. Gap Structure Effects on Surface-Enhanced Raman Scattering Intensities for Gold Gapped Rods. *Nano Lett.* **2010**, *10*, 1722–1727.
2. Alexander, K. D.; Skinner, K.; Zhang, S.; Wei, H.; Lopez, R. Tunable SERS in Gold Nanorod Dimers through Strain Control on an Elastomeric Substrate. *Nano Lett.* **2010**, *10*, 4488–4493.
3. Kang, T.; Yoon, I.; Jeon, K. S.; Choi, W.; Lee, Y.; Seo, K.; Yoo, Y.; Park, Q. H.; Ihee, H.; Suh, Y. D.; *et al*. Creating Well-Defined Hot Spots for Surface-Enhanced Raman Scattering by Single-Crystalline Noble Metal Nanowire Pairs. *J. Phys. Chem. C* **2009**, *113*, 7492–7496.
4. Osberg, K.; Rycenga, M.; Harris, N.; Schmucker, A.; Langille, M. R.; Schatz, G. C.; Mirkin, C. A. Dispersible Gold Nanorod Dimers with Sub-5 nm Gaps as Local Amplifiers for Surface-Enhanced Raman Scattering. *Nano Lett.* **2012**, *12*, 3828–3832.
5. Pucci, A.; Neubrech, F.; Weber, D.; Hong, S.; Toury, T.; Lamy De La Chapelle, M. Surface Enhanced Infrared Spectroscopy using Gold Nanoantennas. *Phys. Status Solidi B* **2010**, *247*, 2071–2074.
6. Han, G.; Weber, D.; Neubrech, F.; Yamada, I.; Mitome, M.; Bando, Y.; Pucci, A.; Nagao, T. Infrared Spectroscopic and Electron Microscopic Characterization of Gold Nanogap Structure Fabricated by Focused Ion Beam. *Nanotechnology* **2011**, *22*, 275202/1–275202/7.
7. Aizpurua, J.; Bryant, G. W.; Richter, L. J.; García de Abajo, F. J.; Kelley, B. K.; Mallouk, T. Optical Properties of Coupled Metallic Nanorods for Feld-Enhanced Spectroscopy. *Phys. Rev. B* **2005**, *71*, 235420/1–235420/13.
8. Willingham, B.; Brandl, D. W.; Nordlander, P. Plasmon Hybridization in Nanorod Dimers. *Appl. Phys. B: Laser Opt.* **2008**, *93*, 209–216.
9. Koh, A. L.; Bao, K.; Khan, I.; Smith, W. E.; Kothleitner, G.; Nordlander, P.; Maier, S. A.; McComb, D. W. Electron Energy-Loss Spectroscopy (EELS) of Surface Plasmons in Single Silver Nanoparticles and Dimers: Influence of Beam Damage and Mapping of Dark Modes. *ACS Nano* **2009**, *3*, 3015–3022.
10. Huang, J. S.; Kern, J.; Geisler, P.; Weinmann, P.; Kamp, M.; Forchel, A.; Biagioni, P.; Hecht, B. Mode Imaging and Selection in Strongly Coupled Nanoantennas. *Nano Lett.* **2010**, *10*, 2105–2110.
11. Liu, M.; Lee, T. W.; Gray, S. K.; Guyot-Sionnest, P.; Pelton, M. Excitation of Dark Plasmons in Metal Nanoparticles by a Localized Emitter. *Phys. Rev. Lett.* **2009**, *102*, 107401/1–107401/4.
12. Alber, I.; Sigle, W.; Müller, S.; Neumann, R.; Picht, O.; Rauber, M.; van Aken, P. A.; Toimil-Molares, M. E. Visualization of Multipolar Longitudinal and Transversal Surface Plasmon Modes in Nanowire Dimers. *ACS Nano* **2011**, *12*, 9845–9853.
13. Atay, T.; Song, J. H.; Nurmikko, A. V. Strongly Interacting Plasmon Nanoparticle Pairs: From Dipole-Dipole Interaction to Conductively Coupled Regime. *Nano Lett.* **2004**, *4*, 1627–1631.
14. Romero, I.; Aizpurua, J.; Bryant, G. W.; García de Abajo, F. J. Plasmons in Nearly Touching Metallic Nanoparticles: Singular Response in the Limit of Touching Dimers. *Opt. Express* **2006**, *14*, 9988–9999.
15. Lassiter, J. B.; Aizpurua, J.; Hernandez, L. I.; Brandl, D. W.; Romero, I.; Lal, S.; Hafner, J. H.; Nordlander, P.; Halas, N. J. Close Encounters between Two Nanoshells. *Nano Lett.* **2008**, *8*, 1212–1218.
16. Schnell, M.; Garcia-Etxarri, A.; Huber, A. J.; Crozier, K.; Aizpurua, J.; Hillenbrand, R. Controlling the Near-Field Oscillations of Loaded Plasmonic Nanoantennas. *Nat. Photonics* **2009**, *3*, 287–291.
17. Pérez-González, O.; Zabala, N.; Borisov, G.; Halas, N. J.; Nordlander, P.; Aizpurua, J. Optical Spectroscopy of Conductive Junctions in Plasmonic Cavities. *Nano Lett.* **2010**, *10*, 3090–3095.
18. Chau, Y. F.; Lin, Y. J.; Tsai, D. P. Enhanced Surface Plasmon Resonance Based on the Silver Nanoshells Connected by the Nanobars. *Opt. Express* **2010**, *18*, 3510–3518.
19. Pérez-González, O.; Zabala, N.; Aizpurua, J. Optical Characterization of Charge Transfer and Bonding Dimer Plasmons in Linked Interparticle Gaps. *New J. Phys.* **2011**, *13*, 083013/1–083013/16.
20. Duan, H.; Hu, H.; Kumar, K.; Shen, Z.; Yang, J. K. W. The Direct and Reliable Patterning of Plasmonic Nanostructures with Sub-10-nm Gaps. *ACS Nano* **2011**, *9*, 7593–7600.
21. Duan, H.; Fernandez-Dominguez, A. I.; Bosman, M.; Maier, S. A.; Yang, J. K. W. Nanoplasmonics: Classical down to the Nanometer Scale. *Nano Lett.* **2012**, *12*, 1683–1689.
22. Large, N.; Abb, M.; Aizpurua, J.; Muskens, O. L. Photoconductively Loaded Plasmonic Nanoantenna as Building Block for Ultracompact Optical Switches. *Nano Lett.* **2010**, *10*, 1741–1746.
23. CST Microwave Studio, http://www.cst.com.
24. García de Abajo, F. J.; Kociak, M. Probing the Photonic Local Density of States with Electron Energy Loss Spectroscopy. *Phys. Rev. B* **2008**, *100*, 106804/1–106804/4.
25. Chu, M. W.; Myroshnychenko, V.; Chen, C. H.; Deng, J. P.; Mou, C. Y.; García de Abajo, F. J. Probing Bright and Dark Surface-Plasmon Modes in Individual and Coupled Noble Metal Nanoparticles Using an Electron Beam. *Nano Lett.* **2009**, *9*, 399–404.
26. Khlebtsov, B. N.; Khlebtsov, N. G. Multipole Plasmons in Metal Nanorods: Scaling Properties and Dependence on Particle Size, Shape, Orientation, and Dielectric Environment. *J. Phys. Chem. C* **2007**, *111*, 11516–11527.
27. Karim, S.; Toimil-Molares, M. E.; Maurer, F.; Miehe, G.; Ensinger, W.; Liu, J.; Cornelius, T. W.; Neumann, R. Synthesis of Gold Nanowires with Controlled Crystallographic Characteristics. *Appl. Phys. A: Mater. Sci. Process* **2006**, *84*, 403–407.
28. Toimil-Molares, M. E.; Brötz, J.; Buschmann, V.; Dobrev, D.; Neumann, R.; Scholz, R.; Schuchert, I. U.; Trautmann, C.; Vetter, J. Etched Heavy Ion Tracks in Polycarbonate as Template for Copper Nanowires. *Nucl. Instrum. Methods Phys. Res. B* **2001**, *185*, 192–197.
29. Toimil-Molares, M. E.; Buschmann, V.; Dobrev, D.; Neumann, R.; Scholz, R.; Schuchert, I. U.; Vetter, J. Single-Crystalline Copper Nanowires Produced by Electrochemical Deposition in Polymeric Ion Track Membranes. *Adv. Mater.* **2001**, *13*, 62–65.
30. Qin, L.; Park, S.; Huang, L.; Mirkin, C. A. On-Wire Lithography. *Science* **2005**, *309*, 113–115.
31. Hoang, N. V.; Kumar, S.; Kim, G. H. Growth of Segmented Gold Nanorods with Nanogaps by the Electrochemical Wet Etching Technique for Single-Electron Transistor Applications. *Nanotechnology* **2009**, *20*, 125607/1–125607/9.
32. Koch, C. T.; Sigle, W.; Höschen, R.; Rühle, M.; Essers, E.; Benner, G.; Matijevic, M. SESAM: Exploring the Frontiers of Electron Microscopy. *Microsc. Microanal.* **2006**, *12*, 506–514.